Theor Chem Acc (2011) 128:735–742
DOI 10.1007/s00214-010-0853-0

REGULAR ARTICLE

Probing vibrational wave packets in molecular excited states

Alberto González-Castrillo · Jhon Fredy Pérez-Torres · Alicia Palacios · Fernando Martín

Received: 27 July 2010 / Accepted: 1 November 2010 / Published online: 21 November 2010

Abstract A time-dependent theoretical method is used to describe a UV pump–UV probe strategy to trace, at a femtosecond time scale, the motion of vibrational wave packets created in excited states of the hydrogen molecule by measuring single ionization probabilities. We use a spectral method to solve the time-dependent Schrödinger equation in full dimensionality, including correlation and all electronic and vibrational degrees of freedom. A pump pulse initially creates a vibrational wave packet in the intermediate electronic excited states of H_2. The frequency of the probe is chosen to ionize the target leaving the ion in a bound vibrational state. By varying the time delay between pulses, non-dissociative single ionization is enhanced or suppressed. Energy differential ionization probabilities are reported and compared with a model based on the Franck–Condon approximation.

Keywords Molecular wave packet · Femtosecond UV pump–UV probe · Multiphoton ionization

Published as part of the special issue celebrating theoretical and computational chemistry in Spain.

A. González-Castrillo · J. F. Pérez-Torres · A. Palacios (✉) · F. Martín
Departamento de Química, Módulo 13, Universidad Autónoma de Madrid, 28049 Madrid, Spain
e-mail: alicia.palacios@uam.es

F. Martín
Instituto Madrileño de Estudios Avanzados en Nanociencias (IMDEA-Nanociencia), Cantoblanco, 28049 Madrid, Spain

1 Introduction

Femtosecond laser technology in the visible and the infrared (IR) has been widely used to understand ultrafast processes in molecules [1–3]. The advent of pump–probe techniques [4] has spurred a large number of works in the last two decades, which has allowed us to gain deep insights into nuclear dynamics, both theoretically [5] and experimentally [6]. Nowadays, the usual procedure consists in using a visible pump pulse to electronically excite the molecule followed by an IR probe pulse to image the nuclear wave packet that is created by the first laser in the excited state of the molecule. The imaging of the wave packet as a function of the time delay between the pump and the probe provides the dynamical information on the nuclear motion in the excited state [7, 8]. Besides imaging the nuclear dynamics, manipulation of the molecule's behavior can be achieved by controlling the pulses characteristics. For example, localization of electrons in simple molecular reactions can be achieved by controlling the carrier envelope phase of such pulses [9]. Recently, the impressive advances in the generation of attosecond XUV pulses have led to the development of new pump–probe schemes, in which the attosecond pulse is used as the pump, thus permitting to trace the electronic dynamics on sub-femtosecond time scales [10, 11]. This has provided unique insight into the nuclear but also on the electronic dynamics in molecules [11].

Very recently, XUV free-electron lasers (FEL) have also come into the play. By using such lasers, a femtosecond XUV pump–XUV probe scheme has been developed to trace the ultrafast nuclear wave packet motion in the D_2^+ molecular ion that is produced by ionizing D_2 with the pump laser [12, 13]. The imaging of the wave packet was possible by detecting the D^+ fragments resulting from the

Coulomb explosion that follows ionization of D_2^+ by the probe laser. In such experiment, the pump and the probe pulses were identical with an energy of 38 eV. A theoretical modeling of such experiments requires the description of two electrons in the continuum in the presence of the two moving deuterons. An accurate description of the double ionization continuum of H_2 (and D_2) has been achieved in the fixed-nuclei and Born–Oppenheimer approximations. These are excellent approximations to describe the double ionization induced by a single photon [14, 15, 16]. However, they are not appropriate to interpret the above-mentioned experiment, because the nuclei have enough time to move before the probe photons are absorbed by the molecule. The lack of accurate theoretical treatments for this particular problem has prevented researchers to obtain a precise conclusion about the relative importance of direct versus sequential double ionization of D_2, as well as about the role of electron correlation in the motion of the wave packet generated by the pump pulse.

In this paper, we propose a different scheme, which is more tractable from the theoretical point of view and can also be realized experimentally by using XUV pulses as those reported in [12, 13]. The pump–probe scheme we propose consists in using a femtosecond XUV pump pulse of 10.9 eV followed by a femtosecond UV probe pulse of 4.6 eV. The sum of the two energies is 15.5 eV, i.e., it is smaller than the energy required to eject both electrons into the continuum. Therefore, the final state is a bound H_2^+ molecular ion plus one electron in the continuum. The dynamics associated with such a final state can be accurately described by solving the time-dependent Schrödinger equation (TDSE) through a close-coupling formalism that includes electron correlation, the nuclear motion and the interferences between them. The method has been successfully employed in previous work [17, 18, 11]. Basically, the idea is that the pump pulse launches a nuclear wave packet in an excited state of H_2, which is then probed by ionizing the molecule with the second pulse. By scanning the time delay between the pump and the probe pulses, we will be able (i) to image the wave packet dynamics in the H_2 electronically excited state, and (ii) to investigate the relative importance of direct versus resonant two-photon single ionization of H_2.

The paper is organized as follows. In Sect. 2, we briefly describe the theoretical method applied, which has been widely explained in earlier publications, see [19, 20] and references therein. Section 3 shows our calculations where the wave packet in the excited state is imaged in the non-dissociative ionization channel. We end with a brief summary of main conclusions. Atomics units are used throughout unless otherwise stated.

2 Methodology

2.1 Time-dependent Schrödinger equation

We work within a semiclassical description where electrons and nuclei are treated quantum mechanically and the laser radiation is written classically, which is a suitable treatment given the intensities used in the present work. We solve the TDSE,

$$i\frac{\partial}{\partial t}\Phi(\mathbf{r},R,t) = H(\mathbf{r},R,t)\Phi(\mathbf{r},R,t) \tag{1}$$

where $\mathbf{r}$ stands for the electronic coordinates (both $\mathbf{r}_1$ and $\mathbf{r}_2$), and R is the internuclear distance. The total Hamiltonian is given as $H(\mathbf{r}, R, t) = H^0(\mathbf{r}, R) + V(\mathbf{r}, R, t)$, with H^0 being the field-free Hamiltonian of the target and $V(t)$ the laser-molecule interaction potential. The Hamiltonian of the hydrogen molecule can be written:

$$H^0(\mathbf{r},R) = T(R) + H_{\mathrm{el}}(\mathbf{r},R) \tag{2}$$

where mass polarization and relativistic correction terms are neglected, $T(R) = -\nabla^2_R/2\mu$ is the nuclear kinetic energy with μ the reduced mass, and H_{el} is the electronic Hamiltonian including the nucleus–nucleus repulsion potential term. Working within the dipole approximation, which is appropriate given the wavelengths hereby considered, the interaction potential is written in the velocity gauge, $V(t) = \mathbf{p}\cdot\mathbf{A}(\mathbf{t})$, in terms of the dipole operator $\mathbf{p}$ and the vector potential $\mathbf{A(t)}$. For a single pulse of photon energy ω and total pulse duration T, $\mathbf{A}(t)$ can be expressed as:

$$\mathbf{A}(t) = \begin{cases} A_0 F(t)\sin(\omega t)\hat{\epsilon} & t\in[0,T] \\ 0 & \text{elsewhere} \end{cases} \tag{3}$$

where $\hat{\epsilon}$ is the polarization vector. We use a sine squared envelope for the time dependence of the pulse $F(t) = \sin^2(\pi t/T)$, whose Fourier transform leads to a spectral frequency bandwidth (i.e., full width at half maximum, FWHM, of the pulse in electric field) $\Delta\omega \approx 4\pi/T$.

In order to solve the TDSE, we use an spectral method using a basis of fully correlated adiabatic vibronic stationary states. The time-dependent wave function $\Phi(\mathbf{r}.R,t)$ in Eq. 1 is expanded in this basis:

$$\begin{aligned} |\Phi(\mathbf{r},R,t)\rangle = &\sum_n \sum\!\!\!\!\!\!\int_{v_n} C_{nv_n}(t)\Psi_{nv_n}(\mathbf{r},R)e^{-iW_{nv_n}t} \\ &+ \sum_\alpha \sum_{\ell_\alpha} \int d\varepsilon_\alpha \sum\!\!\!\!\!\!\int_{v_\alpha} C^{\ell_\alpha}_{\alpha\varepsilon_\alpha v_\alpha}(t)\Psi^{\ell_\alpha}_{\varepsilon_\alpha v_\alpha}(\mathbf{r},R)e^{-iW_{\varepsilon_\alpha v_\alpha}t} \\ &+ \sum_r \sum\!\!\!\!\!\!\int_{v_r} C_{rv_r}(t)\Psi_{rv_r}(\mathbf{r},R)e^{-iW_{rv_r}t} \end{aligned} \tag{4}$$

where $\Psi_{nv_n}(\mathbf{r},R)$ corresponds to the n bound electronic state of H_2 at its v_n (bound or dissociative) vibrational state, $\Psi_{rv_r}(\mathbf{r},R)$ is a resonant electronic state (at its v_r vibrational

state) lying above the ionization threshold, and $\Psi^{\ell_\alpha}_{\varepsilon_\alpha v_\alpha}(\mathbf{r}, R)$ is an electronic continuum state of energy ε_α in the α ionization channel at its v_α (bound or dissociative) vibrational state for an angular momentum l_α of the ejected electron. The symbol $\sum\!\!\!\!\!\!\int$ indicates a summation over bound states plus an integral over the dissociative ones, and W_k is the total energy of each vibronic state.

By inserting expansion (4) in Eq. 1 and projecting into the basis of stationary vibronic states, we obtain a set of coupled linear differential equations. Nonadiabatic couplings are neglected, which is a valid approximation as long as very slow electrons do not play a significant role, as it is in the present case. Time-integration of the system of coupled differential equations is carried out using a Runge–Kutta scheme. Once the field ends, for $t \gg T$, the wave packet is field-free propagated for a given time, to ensure that the asymptotic limit has been reached. Then, ionization amplitudes are extracted by projecting the time-propagated wave packet onto the continuum states. Since the wave packet is written in terms of the stationary states of the system, the expansion coefficients directly give the corresponding amplitudes. Thus, vibrationally resolved ionization probabilities are simply given by:

$$\frac{\mathrm{d}P}{\mathrm{d}E_{v_\alpha}} = \sum_{\ell_\alpha} \int \mathrm{d}\varepsilon_\alpha |C^{\ell_\alpha}_{\alpha\varepsilon_\alpha v_{\varepsilon_\alpha}}(t = T)|^2 \tag{5}$$

where $E_{v_\alpha} = W_{\varepsilon_\alpha v_\alpha} - \varepsilon_\alpha$. For non-dissociative ionization, E_{v_α} is the vibrational energy of the residual H_2^+ ion.

2.2 Stationary states and numerical implementation

Within the Born–Oppenheimer approximation, each vibronic wave function is a product of an electronic and a vibrational function. We first evaluate the electronic states of the hydrogen molecule (bound, continuum and doubly excited states). From the potential energy curves, we then evaluate their corresponding vibrational states. Bound electronic states are obtained by simply solving the eigenvalue problem:

$$H_{\mathrm{el}}\phi_n = \mathcal{E}_n\phi_n \tag{6}$$

Continuum and autoionizing electronic states are described using the Feshbach formalism [21], where two complementary subspaces are defined, $\mathcal{Q}$ containing the resonant contribution and $\mathcal{P} = 1 - \mathcal{Q}$ containing the non-resonant contribution to the electronic wave function. The corresponding wave functions are therefore solutions of:

$$[\mathcal{Q}H_{\mathrm{el}}\mathcal{Q}]\phi_r(\mathbf{r}, R) = \mathcal{E}_r(R)\phi_r(\mathbf{r}, R) \tag{7}$$

$$[\mathcal{P}H_{\mathrm{el}}\mathcal{P}]\phi_{\alpha,l_\alpha,\varepsilon}(\mathbf{r}, R) = \mathcal{E}_{\alpha,\varepsilon}(R)\phi_{\alpha,l_\alpha,\varepsilon}(\mathbf{r}, R) \tag{8}$$

Bound and resonant electronic states, Eqs. 6 and 7, respectively, are obtained within a configuration interaction method using H_2^+ orbitals [22] that are represented in a basis set which is built as products of a radial part, built with 180 B-splines functions of order $k = 8$ in a box of size 60 a.u., and an angular part, written in terms of spherical harmonics with angular momenta up to $l = 16$. Continuum electronic states, Eq. 8, are calculated using a multichannel L^2 close-coupling procedure [23].

The nuclear wave functions $\chi_{v_x}(R)$ are calculated by solving the one-dimensional Schrödinger equation:

$$[T(R) + \mathcal{E}_x(R)]\chi_{v_x}(R) = W_{x,v_x}\chi_{v_x}(R) \tag{9}$$

where x is a bound, resonant or continuum electronic state, and $\mathcal{E}_x$ the corresponding potential energy curve previously obtained. Nuclear wave functions are written in a basis set of 240 B-splines defined in a box of size 12 a.u.

3 Results

We work with linearly polarized light, both parallel and perpendicularly oriented with respect to the molecular axis, in order to obtain any possible contribution to the total ionization probability as it would appear in an experimental setup. For parallel orientations, the dipole selection rules ($\Delta\Lambda = 0$) dictate that only transitions $\Sigma_g \to \Sigma_u \to \Sigma_g$ are permitted; whereas for perpendicular orientation of the molecule with respect to the polarization vector of the electromagnetic field ($\Delta\Lambda = \pm 1$), two different symmetries in the final ionization channels are possible: $\Sigma_g \to \Pi_u \to \Sigma_g$ and $\Sigma_g \to \Pi_u \to \Delta_g$. Overall, spin symmetry of the system must remain singlet as in the initial state of the neutral molecule.

We first excite the molecule with a laser pulse with a photon energy of 0.4 a.u. (10.885 eV) and a duration of 4 fs. Given its energy bandwidth, $\sim$2 eV, this pulse is mainly populating a bunch of vibrational states (around the ten lowest ones) in the first electronic excited state of $^1\Sigma_u^+$ symmetry. The created wave packet then evolves field-free during a given time, after which a second photon of 0.17 au (4.63 eV) and same duration, 4 fs, is absorbed. We use relatively low intensities, 10^9 W cm^{-2} for the first pulse and 10^{12} W cm^{-2} for the second one, to ensure that non linear processes are not dominant. The two-color photon absorption is the main process and leads to non-dissociative ionization. Contributions from other possible mechanisms, as two-photon absorption of two pulses of 0.4 a.u. and 10^9 W/cm^{-2} or four photons of 0.17 a.u. and 10^{12} W cm^{-2}, lead to ionization probability orders of magnitude smaller, therefore negligible, than that of the two-color absorption hereby proposed.

A scheme of the energetics involved in the problem is given in Fig. 1. The sum of the central energies of both

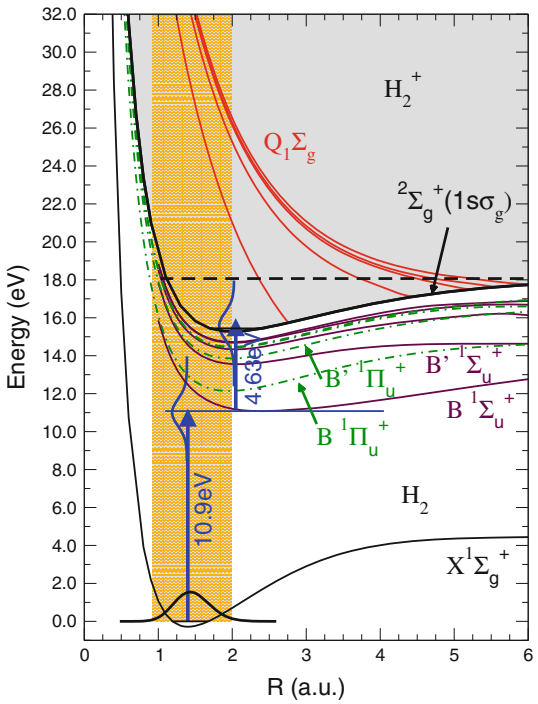

Fig. 1 Potential energy curves of the H_2 molecule. The figure shows the ground state of H_2, the six lowest singly excited states of $^1\Sigma_u^+$ and $^1\Pi_u$ symmetries, the first ionization threshold [i.e., the $^2\Sigma_g^+(1s\sigma_g)$ ground state of H_2^+], and the $^1\Sigma_g^+$ doubly excited states of the Q_1 series of H_2. *The horizontal dashed line* indicates the dissociative limit of the ionization threshold. *The vertical shaded area* is the Franck–Condon associated with the ground state of the molecule

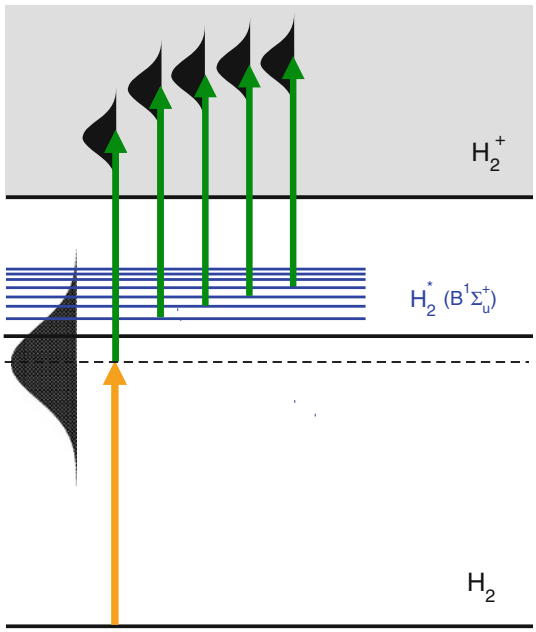

Fig. 2 Simplified scheme on the two-color photo-ionization process. The frequency spectra of the pump pulse contain a range of photon energies that are compatible with the following ionization pathways: (i) direct ionization (DI), in which both photons are simultaneously absorbed (the first photon absorption is possible through "virtual" intermediate states as that shown by the *dashed line*) and (ii) resonant ionization (RI), in which the pump excites the molecule to the $B^1\Sigma_u^+$ excited state and the probe ionizes it from the various vibrational states associated with the latter

pulses (15.515 eV) lies right below the ionization threshold $(E_{v=0}(1s\sigma_g) - E_{v=0}(X^1\Sigma_g^+) = 15.44\,\text{eV})$ in a direct vertical transition. However, within the energy bandwidth of such short pulses, there are two-photon transitions that lead to ionizations and, therefore, to population of the lower vibrational bound states of the ion. The time delay (τ) is measured from the centers of the pulses.

As the two pulses have a duration of 4 fs, simultaneous (direct) absorption of the 0.4 and 0.17 a.u. photons is only possible for delays $0 < \tau < 4$ fs. For $\tau > 4$ fs, the ionization is necessarily achieved by resonant transitions over the intermediate vibronic states populated by the pump pulse. These different pathways are schematically represented in Fig. 2. Ionization by direct two-photon absorption from the ground state is due to a transition through "virtual" intermediate states of the system. Resonant ionization is due to a transition in which the first photon excites the molecule into a vibronic state and the second photon is absorbed from that excite state leading to ionization of the molecule. For time delays longer than 4 fs, the direct two-photon absorption is absolutely suppressed. Both mechanisms are present only in case both pulses overlap in time $(0 < \tau < 4\,\text{fs})$.

In the present study, the pump pulse has been chosen to have a central frequency (maximum amplitude) lower than the energy difference between the first excited state and the ground state of the molecule in a vertical transition (see Figs. 1, 2). Thus, those vibronic states through which two-photon resonant ionization is taking place can only be reached by the few photons whose energy lies in the upper part of the pump spectrum. This choice of pulse parameters should thus favor two-photon direct ionization with respect to resonant ionization (when the former is possible, i.e., $\tau < 4\,\text{fs}$). However, even under these favorable conditions, the contribution of the non-resonant process is negligible. This can be deduced from Fig. 3 (full thick line), where the total ionization probability is plotted as a function of time delay. As it can be seen, in the interval of time delays where both two-photon direct and resonant transitions contribute to ionization $(0 < \tau < 4\,\text{fs})$, the total ionization probability increases with time delay and then it reaches a maximum at 5 fs, where only resonant ionization is possible. The minor contribution of the direct process is not surprising because two-photon resonant ionization probabilities are usually orders of magnitude larger than the two-photon non-resonant ionization ones [24].

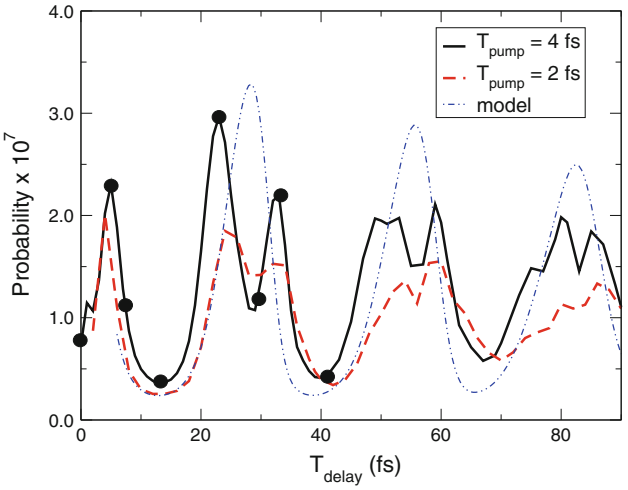

Fig. 3 Ionization probability as a function of time delay for two durations of the pump pulse: 4 fs (*full thick line*) and 2 fs (*dashed line*). The other pump parameters are central photon energy, 10.885 eV, and intensity, 10^9W cm^{-2}. The probe parameters are photon energy, 4.63 eV, intensity 10^{12}Wcm^{-2}, and duration, 4 fs. *Dot-dashed thin line* results of the model explained in the text (a summation over v_k in Eq. 10). *Dots* indicate the time delays for which vibrational distributions are plotted in Fig. 4

The oscillatory pattern observed in Fig. 3 is the signature of the oscillations of the wave packet created by the pump pulse in the $B^1\Sigma_u^+$ excited state. The oscillation period of the ionization probability as a function of time delay is an average of the oscillation periods of the populated bound vibrational states in the $B^1\Sigma_u^+$ electronic state. The estimated (shortest) period for the lowest vibrational state of $B^1\Sigma_u^+$ is $\sim$25 fs, which is of the order of the time difference between peaks, centered at time delays around 5, 25, 55 and 80 fs. Up to approximately ten vibrational states are contained in the wave packet, all of them with different population and phase. Thus, an oscillation period slightly larger than 25 fs is being probed.

For shorter durations of the pump pulse (see Fig. 3, dashed line), the periodicity of the oscillations roughly remains the same, but the profile clearly becomes smoother and the ionization probabilities at the maxima slightly smaller. This is expected because the shorter the pump pulse (i.e. the wider its energy bandwidth), the larger the number of vibrational states contained in the wave packet that is subsequently probed.

It should be mentioned that the range of photon energies contained in the pump pulse is not high enough to populate any electronic excited state of $^1\Pi_u$ symmetry. Thus, the contribution to the ionization signal of perpendicular polarization is less than 2%. Similarly, dissociative ionization is less than 1% of the total ionization probability, because the photon energy is not large enough to reach those states, nor the doubly excited states (although included in the calculations, they do not play any significant role).

As it can be seen in Fig. 3, as time delay increases, the amplitude of the oscillations in the ionization probability decreases. This is an expected behavior due to the spreading of the vibrational wave packet as it evolves in the excited electronic state. For short time delays ($\tau < 5$ fs), the wave packet is mainly localized in the region of internuclear distances associated with a vertical transition from the ground state, i.e., around the equilibrium internuclear distance of H_2 (1.4 a.u.). Whereas for larger time delays, the wave packet has moved and spreads over a range of internuclear distances, which explains the wider structure and smaller amplitude of each oscillation in the ionization probability. A similar decrease and spreading of the ionization probability with time delay has been observed in previous works, as e.g. in pump–probe experiments on D_2 where bound vibrational states of the single ionized molecule were probed using pulses leading to the Coulomb explosion of the system (see Ref. [13]). However, in contrast with the latter study, we find that each oscillation presents an internal structure that becomes more complex as time delay increases. These features, although difficult to interpret, are due to bound-bound transitions between vibrational states of the excited molecule and the ion. The created wave packet contains a bunch of vibronic bound states produced with different relative phases. This is the origin of the increasingly complex internal structure. No structure was observed in [13], because the probe pulse leads to Coulomb explosion, i.e., to the vibrational continuum of H_2^+, which is structureless.

The fact that the probe pulse only leads to non-dissociative ionization is the main reason for the presence of maxima and minima in Fig. 3. Indeed, when the wave packet is localized in the region close to the outer turning point in the potential energy curve of the $^1\Sigma_u^+$ state (internuclear distances around 3–4 a.u.), the ionization probability induced by the probe pulse presents a minimum, since the energy of the probe pulse is not enough to effectively reach the ionization limit at those internuclear distances in a vertical transition (see Fig. 1). In contrast, the ionization probability is maximum in the region close to the inner turning point of the excited electronic state whose vibrational wave packet is being probed. Obviously, we would find maxima associated with both turning points in case the probe led to a dissociative channel, as it is found in the pump–probe experiment reported in [13].

The vibrational wave packet oscillating in the excited state of H_2 leaves a different signature not only in the total, but also in the energy differential ionization probabilities. Fig. 4 shows the vibrational distribution of the remaining H_2^+ in the ground electronic state, $^2\Sigma_g^+(1s\sigma_g)$, at different

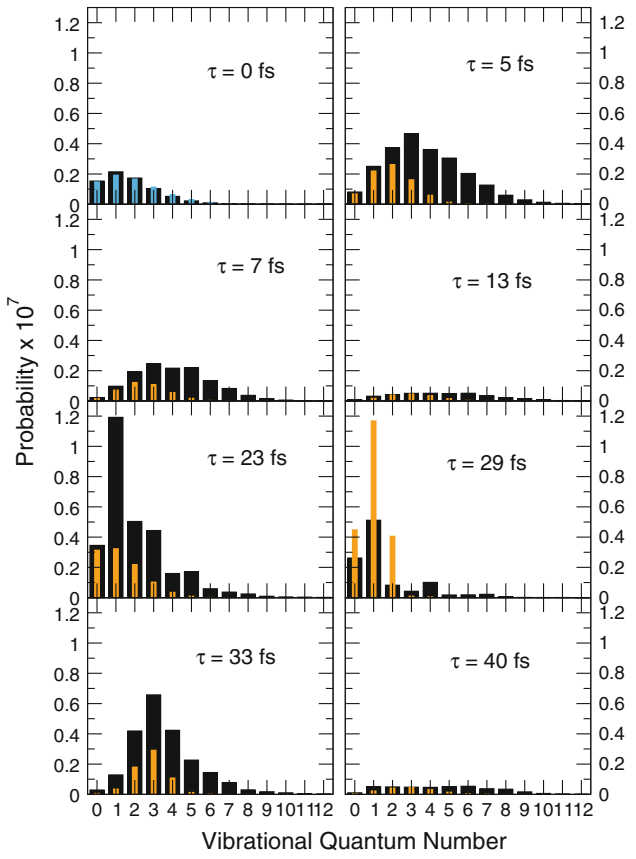

Fig. 4 H_2^+ vibrational distributions for a pump pulse of 4 fs and the time delays indicated by *full dots* in Fig. 3. *Black thick bars* ab initio present calculations. *Orange thin bars* results from the model (renormalized). *Blue thin bars* for the panel at zero time delay: Frank–Condon overlap with the ground state of H_2 multiplied by the vector potential of the probe in the energy domain

time delays between the pulses. The distributions plotted in Fig. 4 correspond to the time delays indicated with black circles in Fig. 3. For zero time delay, the probability distribution is almost identical to that obtained by a direct vertical transition from the ground state convoluted with the Fourier transform of the probe pulse. This comparison is shown in the top left panel in Fig. 4. At zero time delay, the molecule has no time to vibrate, the created wave packet has no time to evolve, and consequently, the transition will proceed roughly in the Frank-Condon region delimited by the ground state of the neutral. For time delays larger than 4 fs, ionization necessarily takes place through two-photon resonant absorption where the second pulse probes the wave packet created by the pump pulse. Consequently, the vibrational distribution of H_2^+ reveals the features of the field-free evolution of the wave packet in the excited state of H_2. For a time delay of 5 fs (corresponding to the first maximum in Fig. 3), the wave packet has had enough time to move towards slightly larger internuclear distances, thus increasing the overlap with the bound vibronic states of the ion (the equilibrium distance of H_2^+ is 2.0 a.u.). This leads to larger ionization yields and shifts the vibrational distribution to higher vibrational states with respect to those obtained without delay. For those time delays where we find a minimum in the total ionization probability, $\tau = 13$ and 40 fs, the ionization probability is rather uniform for the ten lowest vibrational states of the ion. These wide distributions reflect the oscillating wave packet being spread out in the excited state when the probe pulse is absorbed. On the other hand, for time delays leading to the larger total ionization probabilities, $\tau = 23$ and 33 fs, the wave packet is localized at the inner turning point thus favoring the overlap with the bound vibronic states of the ion, as it is shown in the two lower left panels in Fig. 4.

In Fig. 4, the results of the ab initio calculations are compared with those from a simple model in which probabilities are obtained by projecting onto the final vibronic states the wave packet that is created at the end of the pump pulse and has evolved field-free up to the corresponding time delay. This is equivalent to perform the Frank-Condon approximation to describe the photon absorption induced by the probe pulse. Thus, electronic dipole couplings and correlations are totally ignored in this model, in which the vibrational distribution probabilities are given by the expression:

$$P_{v_\alpha} = \left| \sum_{v_i} c_{v_i}(t = T_1) e^{-i(W_{i,v_i} - W_{\alpha,v_\alpha})\Delta t/\hbar} \langle \chi_{v_\alpha} | \chi_{v_i} \rangle F_{v_\alpha} A(t) \right|^2 \tag{10}$$

where $\sum_{v_i}$ is the summation over those bound vibrational states χ_{v_i} that are effectively populated by the pump pulse in the $B^1\Sigma_u^+$ electronic state, W_{i,v_i} and W_{α,v_α} are, respectively, the total (vibrational + electronic) energy of the excited and final states, $\Delta t = \tau - T/2$ (i.e., taking the vertical transition at the center of the probe pulse, when it reaches its maximum field amplitude), and $c_{v_i}(t = T_1)$ are the expansion coefficients of the excited states contained in the wave packet at the end of the pump pulse. To take into account the pulse shape and duration, the Franck–Condon overlap $\langle \chi_{v_\alpha} | \chi_{v_i} \rangle$ is convoluted with the Fourier transform of the vector potential $A(t)$: $F_{v_\alpha} A(t)$. The probabilities obtained with this model have been renormalized to fit ab initio calculations, using the same arbitrary factor for all vibrational distributions.

The vibrational distributions obtained with the model agree qualitatively with those of the ab initio calculations. The disagreements mainly come from the R-dependence and the phases of the dipole transition moments and from electronic correlations, which are totally neglected in the model. As shown in Fig. 3 (dotted-dashed thin line), the

model also reproduces quite nicely the oscillations as a function of time delay (in the model, the total ionization probability has been obtained as $\sum_{v_\alpha} P_{v_\alpha}$). The complex internal structure in the oscillations cannot be reproduced by the model, because the appropriate relative phases of the different bound-bound transitions that lead to the created wave packet are not taken into account.

4 Conclusions

Ab initio calculations are reported for non-dissociative single ionization of H_2 through a UV pump–UV probe scheme, in which the nuclear wave packet created by the pump pulse in the excited states of the molecule is traced by the probe pulse. An accurate description of such process unavoidable requires a time-dependent treatment accounting for both nuclear and electronic motions, since the vibration of the nuclei in the intermediate excited states of H_2 periodically enhances or suppresses ionization. The oscillation of the ionization probability as a function of the time delay between the two pulses reflects the oscillation of the vibrational wave packet in the excited state of the molecule. Two-photon direct absorption is almost negligible, even though two-photon resonant ionization is only accessible by photons whose energy lies in the upper region of the pulse spectrum. The vibrational distributions of the ion are the signature of the wave packet created by the pump. Minima in total ionization yields correspond to wide vibrational distributions, reflecting the spreading of the wave packet. The maxima in the ionization probabilities result from the more efficient population of the few lower vibrational bound states of the ion, which is due to localization of the probed wave packet in the region of short internuclear distances. A simple model based on the Frank–Condon approximation for the second photon absorption qualitatively reproduces the oscillations of the total ionization probability as a function of time delay and, to a lesser extent, the corresponding vibrational distributions of the ion.

Acknowledgments We thank Mare Nostrum BSC and CCC-UAM for allocation of computer time. Work partially supported by the European COST Action CM0702 and Ministerio de Ciencia e Innovación through the DGI projects Nos. FIS2007-60064 and CSD 2007-00010 and the DGCI project No. ACI2008-0777. AP gratefully acknowledges a Juan de la Cierva post-doctoral contract from the Ministerio de Ciencia e Innovación of Spain.

References

1. Bandrauk AD, Manz J, Vrakking MJJ (2009) Chem Phys 366(1–3):1. doi:10.1016/j.chemphys.2009.10.023. http://www.sciencedirect.com/science/article/B6TFM-4XKHDD0-1/2/061ec6a5fc5a0da2649d48db06bda75a. Attosecond Molecular Dynamics
2. Calvert CR, King RB, Bryan WA, Newell WR, McCann JF, Greenwood JB, Williams ID (2010) J Phys B At Mol Opt Phys 43(1):011001. http://stacks.iop.org/0953-4075/43/i=1/a=011001
3. Kelkensberg F, Lefebvre C, Siu W, Ghafur O, Nguyen-Dang TT, Atabek O, Keller A, Serov V, Johnsson P, Swoboda M, Remetter T, L'Huillier A, Zherebtsov S, Sansone G, Benedetti E, Ferrari F, Nisoli M, Lépine F, Kling MF, Vrakking MJJ (2009) Phys Rev Lett 103(12):123005
4. Mokhtari A, Cong P, Herek JL, Zewail AH (1990) Nature 348:225
5. Meier C, Engel V (1993) Chem Phys Lett 212(6):691. doi:10.1016/0009-2614(93)85506-J. http://www.sciencedirect.com/science/article/B6TFN-44WCVS0-3G/2/52e08f68d17a2261d53e2da7352b17ea
6. Assion A, Geisler M, Helbing J, Seyfried V, Baumert T (1996) Phys Rev A 54(6):R4605
7. Ergler T, Rudenko A, Feuerstein B, Zrost K, Schröter CD, Moshammer R, Ullrich J (2006) Phys Rev Lett 97(19):193001
8. Brinks D, Stefani FD, Kulzer F, Hildner R, Taminiau TH, Avlasevich Y, Mullen K, van Hulst NF (2010) Nature 465:905–908. doi:10.1038/nature09110. http://dx.doi.org/10.1038/nature09110
9. Krausz F, Ivanov M (2009) Rev Mod Phys 81(1):163
10. Gagnon E, Ranitovic P, Tong X, Cocke CL, Murname MM, Kapteyn HC, Sandhu AS (2007) Science 317(5843):1374. doi:10.1126/science.1144920
11. Sansone G, Kelkensberg F, Perez-Torres JF, Morales F, Kling MF, Siu W, Ghafur O, Johnsson P, Swoboda M, Benedetti E, Ferrari F, Lepine F, Sanz-Vicario JL, Zherebtsov S, Znakovskaya I, L'Huillier A, Ivanov MY, Nisoli M, Martin F, Vrakking MJJ (2010) Nature 465:763. doi:10.1038/nature09084. http://dx.doi.org/10.1038/nature09084
12. Jiang YH, Rudenko A, Pérez-Torres JF, Herrwerth O, Foucar L, Kurka M, Kühnel KU, Toppin M, Plésiat E, Morales F, Martín F, Lezius M, Kling MF, Jahnke T, Dörner R, Sanz-Vicario JL, van Tilborg J, Belkacem A, Schulz M, Ueda K, Zouros TJM, Düsterer S, Treusch R, Schröter CD, Moshammer R, Ullrich J (2010) Phys Rev A 81(5):051402. doi:10.1103/PhysRevA.81.051402
13. Jiang YH, Rudenko A, Plésiat E, Foucar L, Kurka M, Kühnel KU, Ergler T, Pérez-Torres JF, Martín F, Herrwerth O, Lezius M, Kling MF, Titze J, Jahnke T, Dörner R, Sanz-Vicario JL, Schöffler M, van Tilborg J, Belkacem A, Ueda K, Zouros TJM, Düsterer S, Treusch R, Schröter CD, Moshammer R, Ullrich J (2010) Phys Rev A 81(2):021401. doi:10.1103/PhysRevA.81.021401
14. Vanroose W, Martín F, Rescigno TN, McCurdy CW (2004) Phys Rev A 70(5):050703. doi:10.1103/PhysRevA.70.050703
15. Vanroose W, Martín F, Rescigno TN, McCurdy CW (2005) Science 310(5755):1787. doi:10.1126/science.1120283
16. Horner DA, Vanroose W, Rescigno TN, Martín F, McCurdy CW (2007) Phys Rev Lett 98(7):073001. doi:10.1103/PhysRevLett.98.073001
17. Pérez-Torres JF, Sanz-Vicario JL, Bachau H, Martín F (2010) J Phys B At Mol Opt Phys 43(1):015204. http://stacks.iop.org/0953-4075/43/i=1/a=015204
18. Morales F, Pérez-Torres JF, Sanz-Vicario JL, Martín F (2009) Chem Phys 366(1–3):58. doi:10.1016/j.chemphys.2009.09.008 http://www.sciencedirect.com/science/article/B6TFM-4X6FNPF-1/2/ac4577a76c27be6231f7cb1f0f48d0da. Attosecond Molecular Dynamics
19. Sanz-Vicario JL, Bachau H, Martín F (2006) Phys Rev A 73:033410
20. Sanz-Vicario JL, Palacios A, Cardona JC, Bachau H, Martín F (2007) J Electron Spectros Relat Phenomena 161:182

21. Feshbach H (1962) Ann Phys 19:287
22. Bachau H, Cormier E, Decleva P, Hansen JE, Martín F (2001) Rep Prog Phys 64(12):1815. http://stacks.iop.org/0034-4885/64/i=12/a=205
23. Cortés M, Martín F (1994) J Phys B At Mol Opt Phys 27(23):5741. http://stacks.iop.org/0953-4075/27/i=23/a=017
24. Palacios A, Bachau H, Martín F (2007) Phys Rev A 75(1):013408. doi:10.1103/PhysRevA.75.013408